

# Interpreting BERT-based Text Similarity via Activation and Saliency Maps

Itzik Malkiel\*  
Microsoft  
Tel-Aviv University  
Israel

Dvir Ginzburg\*  
Microsoft  
Tel-Aviv University  
Israel

Oren Barkan  
The Open University  
Microsoft  
Israel

Avi Caciularu  
Bar-Ilan University  
Israel

Jonathan Weill  
Microsoft  
Israel

Noam Koenigstein  
Microsoft  
Tel-Aviv University  
Israel

## ABSTRACT

Recently, there has been growing interest in the ability of Transformer-based models to produce meaningful embeddings of text with several applications, such as text similarity. Despite significant progress in the field, the explanations for similarity predictions remain challenging, especially in unsupervised settings. In this work, we present an unsupervised technique for explaining paragraph similarities inferred by pre-trained BERT models. By looking at a pair of paragraphs, our technique identifies important words that dictate each paragraph's semantics, matches between the words in both paragraphs, and retrieves the most important pairs that explain the similarity between the two. The method, which has been assessed by extensive human evaluations and demonstrated on datasets comprising long and complex paragraphs, has shown great promise, providing accurate interpretations that correlate better with human perceptions.

## CCS CONCEPTS

• **Computing methodologies** → **Machine Learning, Natural Language Processing**; • **Information systems** → **Presentation of retrieval results**.

## KEYWORDS

Self-supervised, Deep Learning, Transformers, Attention Models, Explainable AI, Interpretability

## ACM Reference Format:

Itzik Malkiel, Dvir Ginzburg, Oren Barkan, Avi Caciularu, Jonathan Weill, and Noam Koenigstein. 2022. Interpreting BERT-based Text Similarity via Activation and Saliency Maps. In *Proceedings of the ACM Web Conference*

\*Both authors contributed equally to this research.

Permission to make digital or hard copies of all or part of this work for personal or classroom use is granted without fee provided that copies are not made or distributed for profit or commercial advantage and that copies bear this notice and the full citation on the first page. Copyrights for components of this work owned by others than ACM must be honored. Abstracting with credit is permitted. To copy otherwise, or republish, to post on servers or to redistribute to lists, requires prior specific permission and/or a fee. Request permissions from [permissions@acm.org](mailto:permissions@acm.org).

WWW '22, April 25–29, 2022, Virtual Event, Lyon, France

© 2022 Association for Computing Machinery.

ACM ISBN 978-1-4503-9096-5/22/04...\$15.00

<https://doi.org/10.1145/3485447.3512045>

2022 (WWW '22), April 25–29, 2022, Virtual Event, Lyon, France. ACM, New York, NY, USA, 10 pages. <https://doi.org/10.1145/3485447.3512045>

## 1 INTRODUCTION

The increasing availability of artificial intelligence systems has brought about an increasing demand for methods to intuitively explain machine inference and predictions [2, 24, 42]. Machine explanations are utilized for a multiplicity of applications. From increasing users' trust [9, 27, 38] and improving interpretability [4, 10, 19, 20, 24] to debugging [31]. In some cases, explanations are used to enhance the autonomy of people and facilitate direct oversight of algorithms [18]. As a result, some countries have regulations that make explanations mandatory in sensitive cases [29, 41].

Transformer-based models have revolutionized the fields of natural language processing [22, 33, 46] and recommender systems [34, 44], improving upon other neural embedding models [3, 5, 7, 8, 13–15, 17, 36, 37, 40]. Significant strides were made in tasks such as machine translation [46], sentiment analysis [49], semantic textual similarity [16, 23, 35], and item similarity [6, 11, 12, 28, 34]. However, transformers employ a complex attention-based architecture comprising hundreds of millions of parameters that cannot be decomposed into smaller more interpretable components. Hence, explaining transformer-based models is still an open question.

In this paper, we present BTI - a novel technique for explaining unlabeled paragraph similarities inferred by a pre-trained BERT model. BTI produces interpretable explanations for the similarity of two textual paragraphs. First, both paragraphs are propagated through a pre-trained BERT model, yielding contextual paragraph representations. A similarity score such as the cosine similarity is used to measure the affinity between the paragraphs. Gradient maps for the first paragraph's embeddings are calculated w.r.t. the similarity to the second paragraph. These gradient maps are scaled by multiplication with the corresponding activation maps and summed across the feature dimensions to produce a saliency score for every token in the first paragraph. The token saliency scores are then aggregated to words, yielding word scores.

Next, BTI performs the same procedure, with the first paragraph and second paragraphs reversed. This yields word scores for the second paragraph, calculated w.r.t to the similarity with the first. Finally, the algorithm matches word-pairs from both paragraphs,

scoring each pair by the importance scores associated with its elements and the similarity score associated with the pair. The most important word-pairs are then detected and retrieved as explanations.

Our contributions are as follows: (1) we present BTI, a novel method for interpreting paragraph similarity in unlabeled settings. (2) we show the effectiveness of BTI in explaining text similarity on two datasets and demonstrate its ability to pass a common sanity test. (3) we compare BTI with other alternatives via extensive human evaluations, showcasing its ability to better correlate with human perception.

## 2 RELATED WORK

A seminal breakthrough in visualization and interpretation of deep neural networks was presented in [51]. In this work, the authors proposed to employ the deconvolution operations [52] on the activation maps w.r.t. the input image, generating visual features to interpret model predictions.

A different approach was employed by [43, 50] where guided backpropagation (GBP) was proposed as an explanation method that is not restricted to visual classification models. GBP visualizes the output prediction by propagating the gradients through the model and suppressing all negative gradients along the backward pass, resulting in saliency maps of the most influenced input parts w.r.t. the downstream task.

To test the reliability of common explainability methods, Adedayo et al. [1] proposed the parameter randomization test. The test suggests propagating the same input through a pre-trained and randomly initialized network to estimate the method’s dependence on the underlying network weights. The proposed sanity check reveals that most of the methods described above do not pass the test, i.e., they are independent of the model parameters and therefore are not adequate for providing satisfactory model explanations. In Section 4.1, we show that BTI passes those important sanity checks.

Based on these canonical works, the NLP community introduced interpretability tools for architectures other than CNNs. The first works that proposed interpretation of textual-based networks include [32], and [39]. In [32], the authors offer to justify model predictions by generating important fragments of the inputs. Their technique utilizes explanations during training, integrating an encoder-generator paradigm that can be used to predict explanations during inference. In [39] the authors propose a “black-box” classifier interpretability using local perturbation to the input sequence to explain the prediction. However, since both methods rely on supervision, they can not be employed in unlabeled settings.

Another vast problem of explainability methods for NLP tasks is the variation of the input length. To adhere to this problem, the authors in [53] use a Variational Autoencoder for the controlled generation of input perturbations, finding the input-output token pairs with the highest variation. While several authors adopted the sequence-pair explainability scheme, they only tackle input-output relations, hence incompatible for unlabeled text-similarity tasks.

Since the emergence of the transformer architecture [46], several groups have tried to offer interpretation techniques for the models.

exBERT [30], for example, published a visual analysis tool for the contextual representation of each token based on the attention weights of the transformer model. AllenNLP Interpret [47] offers token-level reasoning for BERT-based classification tasks such as sentiment analysis and NER using published techniques such as HotFlip [25], Input Reduction [26] or vanilla gradients analysis.

In integrated gradients (IG) [45], the authors propose an explainability method that approximates an integral of gradients of the model’s output w.r.t. the input. To this end, IG generates a sequence of samples by interpolating the input features with 0, computing gradients for each sample in the sequence, and approximating an integral over the produced gradients. The integral is then used to score the importance of each input feature. The authors of SmoothGrad proposed a similar yet simpler technique, by feed-forwarding noisy versions of the input, and averaging the gradients of the different outputs with respect to the objective function.

## 3 METHOD

In this section, we present the mathematical setup of BTI and its applications for explainable text-similarity in self-supervised pre-trained language models. We build our method upon BERT, however, BTI can be applied with other Transformer-based language models.

### 3.1 Problem Setup

Let  $\mathcal{V} = \{t_i\}_{i=1}^V$  be the vocabulary of words in a given language. Let  $S$  be the set of all possible sentences induced by  $\mathcal{V}$ . Additionally, let  $P$  be the set of all possible paragraphs generated by  $S$ .

BERT can be defined as a function  $B : P \rightarrow \mathbb{R}^{N \times h}$ , where  $h$  is the hidden layer size, and  $N = 512$  is the maximal sequence length supported by the model. In inference, BERT receives a paragraph  $p \in P$  and decomposes it into a sequence of  $q \in \mathbb{N}$  tokens  $(p^j)_{j=1}^q$ , by utilizing the WordPiece model [48]. The sequence is then wrapped and padded to  $N$  elements, by adding the special *CLS*, *SEP* and *PAD* tokens. This token sequence can be written as  $IP := (CLS, (p^j)_{j=1}^q, SEP, \dots, PAD)$ .

In BERT, all tokens are embedded by three learned functions: token, position and segment embeddings, denoted by  $T$ ,  $O$ , and  $G$ , respectively. The token embedding transforms tokens’ unique values into intermediate vectors  $T(IP) \in \mathbb{R}^{N \times h}$ . The position embedding encodes the token positions to the same space,  $O(IP) \in \mathbb{R}^{N \times h}$ . The segment embedding is used to associate each token with one out of two sentences  $G(\{0, 1\}^N) \in \mathbb{R}^{N \times h}$  (as standard BERT models are trained by sentence pairs).

In this work, we feed BERT with single paragraphs and leave the use of paragraph-pairs sequences to future investigation. The principle behind this choice stems from two aspects: (1) in many cases, paragraph similarity labels do not exist, therefore, we can not fine-tune the language model to the task of paragraph-pairs similarity. This entails the use of a pre-trained language model, that is commonly trained by sentence pairs or chunks of continuous text, and does not specialize in non-consecutive paragraph pairs. Therefore, the inference of non-consecutive paragraph-pairs may introduce instabilities, due to the discrepancy between both phases.

**Algorithm 1** BTI algorithm. The MeanShift function returns the cluster index for each sample. The clusters are sorted in descending order w.r.t. to their centroids (i.e. the top-performing cluster receives the index 0). Params:  $top\_k = 2, p_1, p_2 \in P$ .

```

function MATCHWORDS( $\widehat{w}^1, \widehat{w}^2, w_s^1, w_s^2, w^1, w^2$ , reversed)
   $M := \{\}$ 
  for  $1 \leq i \leq |\widehat{w}^1|$  do
     $m, c \leftarrow 1, C(\widehat{w}_i^1, \widehat{w}_1^2)$ 
    for  $2 \leq j \leq |\widehat{w}^2|$  do
       $\widehat{c} \leftarrow C(\widehat{w}_i^1, \widehat{w}_j^2)$ 
      if  $c \leq \widehat{c}$ :  $m, c \leftarrow j, \widehat{c}$ 
    end for
    if reversed then
       $M \leftarrow M \cup \{((w_m^2, w_i^1), (w_s^1)_i \cdot (w_s^2)_m \cdot c)\}$ 
    else
       $M \leftarrow M \cup \{((w_i^1, w_j^2), (w_s^1)_i \cdot (w_s^2)_m \cdot c)\}$ 
    end if
  end for
  return  $M$ 
end function

1:  $s^1 := (s_j^1)_{j=1}^m \leftarrow \text{TokenSaliency}(p_2, p_1)$ 
2:  $s^2 := (s_j^2)_{j=1}^m \leftarrow \text{TokenSaliency}(p_1, p_2)$ 
3:  $w^1, \widehat{w}^1, w_s^1 = \text{WordPiece}^{-1}(p_1, B(p_1), s^1)$ 
4:  $w^2, \widehat{w}^2, w_s^2 = \text{WordPiece}^{-1}(p_2, B(p_2), s^2)$ 
5:  $m^1 \leftarrow \text{MatchWords}(\widehat{w}^1, \widehat{w}^2, w_s^1, w_s^2, w^1, w^2, \text{False})$ 
6:  $m^2 \leftarrow \text{MatchWords}(\widehat{w}^2, \widehat{w}^1, w_s^2, w_s^1, w^1, w^2, \text{True})$ 
7: return  $\text{TopWords}(m^1, m^2, top\_k)$ 

function  $F_p(p)$ 
   $F_p \leftarrow \frac{1}{|p|} \sum_{i=2}^{|p|+1} B(p)_i$ 
  return  $F_p$ 
end function

function TOKENSALIENCY( $p_1, p_2$ )
   $g \leftarrow \frac{\partial C(F_{p_1}, F_{p_2})}{\partial E(p_2)}$ 
   $s \leftarrow \left[ \sum_{k=1}^h \phi(E(p_2)_i \circ (g_i)_k) \right]_{i=1}^{|p_2|}$ 
   $s \leftarrow \text{min-max}(s)$ 
  return  $s$ 
end function

function TOPWORDS( $m^1, m^2, top\_k$ )
   $M \leftarrow m^1 \cup m^2$ 
   $M^* \leftarrow ((M_j)_2)_{j=1}^{|M|}$  ▷ word-pair scores
   $S := (c)_{c=1}^{|m^1|+|m^2|} \leftarrow \text{MeanShift}(M^*)$  ▷ the cluster index
  for each sample
     $T := \{\}$ 
    for  $1 \leq i \leq |M|$  do
       $T \leftarrow T \cup \{M_i\}$ , if  $S_i \leq top\_k$ 
    end for
  return  $T$ 
end function

```

(2) the technical limitation of maximal sequence length in BERT architecture, for which feeding two paragraphs as a unified sequence may exceed the limit of 512 tokens.

### 3.2 BERT Interpretations (BTI)

By propagating  $p$  through BERT, the model produces a sequence  $B(p) \in \mathbb{R}^{N \times h}$  of latent tokens. Each element in  $B(p)$  is associated with its matched element in  $I^p$ . A feature vector can be computed for each paragraph by average pooling the output tokens as follows:

$$F_p := \frac{1}{q} \sum_{i=2}^{q+1} B(p)_i, \quad (1)$$

omitting the latent elements associated with the *CLS*, *SEP* and *PAD* input tokens.

The similarity between paragraph-pairs can be interpreted by highlighting and matching important words from each element. The highlighted words in both elements should dictate the semantical similarity of the two paragraphs in a way that correlates with human perception. Hence, given two paragraphs denoted by  $p_1 \in P$  and  $p_2 \in P$ , we build BTI to identify important word-pairs with

similar semantics  $M := \{(x_i, y_i)\}_{i=1}^e$ , where  $x_i \in p_1$  and  $y_i \in p_2$ , for all  $i$ , and  $e$  is the number of pairs detected by BTI.

Since each paragraph is fed as a separate sequence, we build our method upon the  $T$  and  $O$  embeddings. Specifically, given the paragraphs  $p_1$  and  $p_2$ , BTI first calculates saliency maps, for each paragraph, by utilizing the activation map values  $E(I^{p_1}) \in \mathbb{R}^{q_1 \times h}$  and  $E(I^{p_2}) \in \mathbb{R}^{q_2 \times h}$  where

$$E(I^p) := T(I^p) + O \left( (i)_{i=1}^N \right) \quad (2)$$

along with the gradients calculated on the same activations w.r.t. to a cosine score between the feature vectors of both paragraphs.  $q_1$  and  $q_2$  denote the number of tokens in the WordPiece decomposition of  $p_1$  and  $p_2$ , respectively.

The BTI algorithm is depicted in Alg.1. In lines 1-2, BTI invokes the TokenSaliency function to infer a *token-saliency* score for each token in the given paragraph-pair. The TokenSaliency is first applied to  $(p_1, p_2)$ , then, in line 2, the roles of  $p_1$  and  $p_2$  are reversed. Since both sides are analogue, we will describe TokenSaliency by its first application. For a given paragraph pair  $(p_1, p_2)$ , the function propagates each paragraph through BERT, calculates the feature vectors  $F_{p_1}, F_{p_2}$  and

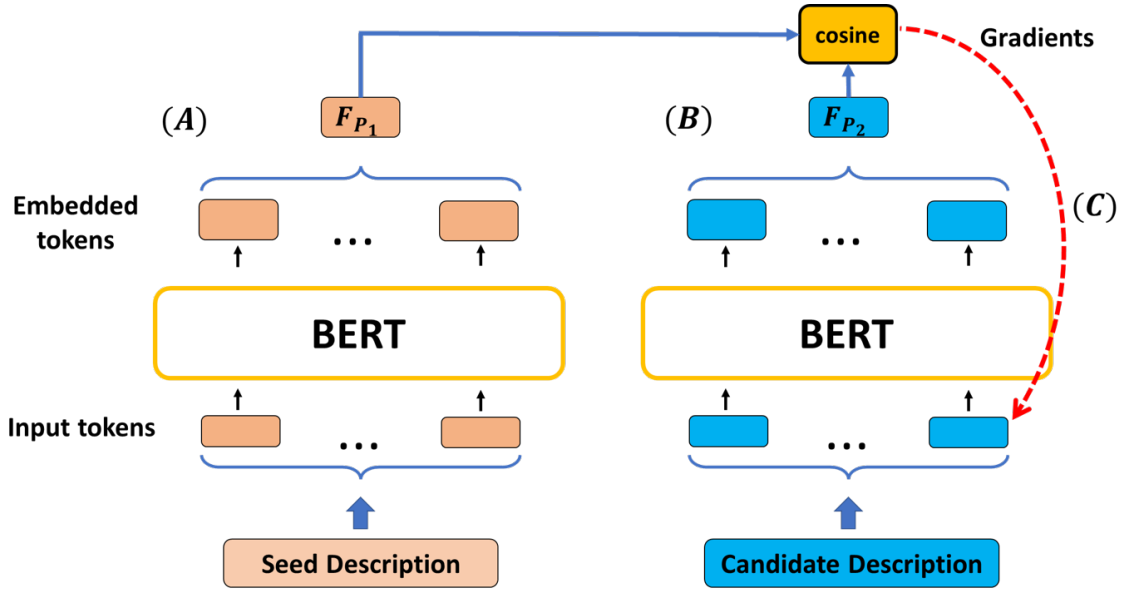


**Figure 1: Illustration of the gradient calculation w.r.t. the similarity between two bodies of text. (A) the description of the seed item is propagated through the model, which then outputs embeddings that are averaged pooled into a single feature vector. (B) the same procedure is applied to the description of the candidate item, where the model retrieves a feature vector that represents the candidate text. (C) a similarity function, such as the cosine similarity, is applied between both vectors, followed by a gradients calculation on the input embeddings of the candidate text w.r.t. to the similarity score. The same procedure is applied twice, where the roles of the seed and the candidate text are reversed (not shown in the figure).**

the partial derivations,  $g(p_1, p_2) \in \mathbb{R}^{N \times q_2}$ , of the input embeddings  $E(I^{p_2})$  w.r.t. to the cosine between the two feature vectors  $F_{p_1}$  and  $F_{p_2}$  (the first feature vector is used as a constant, the second is generated by propagating  $p_2$  through the model to derive gradients on its intermediate representations). Formally:

$$g(p_1, p_2) := \frac{\partial C(F_{p_1}, F_{p_2})}{\partial E(p_2)} \quad (3)$$

where  $C$  is a similarity function. In our experiments we utilize the cosine similarity function<sup>1</sup>. Importantly, the positive gradients of the above term are the ones that maximize the cosine similarity between the two paragraphs (whereas stepping towards the direction of the negative gradients, would entail a smaller cosine similarity). An illustration of this gradients calculation can be seen in Fig. 1. For completeness, we also provide a figure demonstrating the effectiveness of the gradients, calculated on a representative sample of seed-candidate descriptions. In Fig. 2 we present the gradients' norm calculated on the words of a given candidate description w.r.t. to the similarity with its matched seed description.

The gradients are then multiplied by the activation maps of the same embeddings:

$$s = \text{NRM} \left[ \left( \sum_{k=1}^h \phi(E(p_2)_i \circ g_i)_k \right)_{i=1}^{q_2} \right] \quad (4)$$

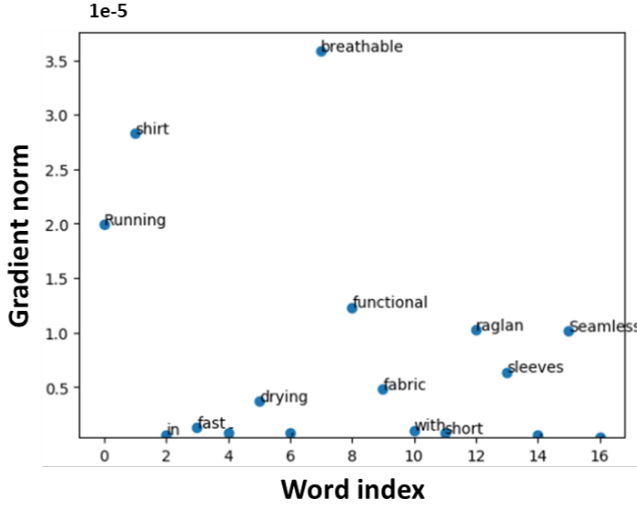
<sup>1</sup> $C(v, u) = \frac{v \cdot u}{\|v\| \|u\|}$  where  $v, u \in \mathbb{R}^h$

where  $\phi$  is the ReLU activation function,  $\circ$  is the Hadamard product, and NRM is the min-max normalization, which transforms the data to  $[0, 1]$ .

The motivation behind Eq. 4 is as follows: we expect important tokens to have embedding values and gradients that agree in their sign - namely both positive or both negative. This indicates that the gradients that stem from  $C(F_{p_1}, F_{p_2})$  emphasize the relevant parts of the embeddings that are important for the similarity between the two paragraphs. Additionally, embeddings and gradients with higher absolute values are more significant than those with values near zero.

In line 3-4, BTI applies the  $\text{WordPiece}^{-1}$  function. This function receives (1) the tokens, (2) the latent token representations<sup>2</sup>, and (3) the token-saliency scores of a given paragraph. The function then aggregates all arguments to word-level representation, retrieving (1) whole words (rebuilt from tokens), (2) latent representation for each word, and (3) word-saliency scores. The second and third aggregations employ predefined functions  $\varphi$  and  $\psi$  on the latent tokens and token-saliency scores associated with the same word, respectively. The result word-level representation is then retrieved as an output.  $w^1$  and  $w^2$  denote the words sequences produced by aggregating the tokens of  $p_1$  and  $p_2$ , respectively.  $\widehat{w}^1$  and  $\widehat{w}^2$  denote the aggregated latent word-level representation of  $p_1$  and

<sup>2</sup>generated by propagating the paragraph through BERT



Seed description: “Sleeveless sports shirt in fast-drying functional fabric with taped details. Rounded hem, slightly longer at back.”

Candidate description: “Running shirt in fast-drying, breathable functional fabric with short raglan sleeves Seamless.”

**Figure 2: A visualization of the gradients norm of a representative candidate description calculated w.r.t. its cosine similarity with its seed item. The words associated with the highest gradient norm are considered to be the most important words in the candidate’s textual description. The seed description and candidate description appear at the bottom of the graph.**

$p_2$ , respectively. Analogously, the word-saliency scores are denoted by  $w_s^1$  and  $w_s^2$ .

In our experiments, we define  $\varphi$  and  $\psi$  as the mean and max functions. This entails that (a) the latent representation of a word would be defined by the mean representation of its tokens, and (b) the importance of a given word would be matched to the maximal importance of its tokens. For example, assuming a given paragraph comprising the word “playing”, for which the BERT tokenizer decomposes the word to the tokens “play” and “ing”. Assuming the TokenSaliency function assigns the tokens with the token-saliency scores 0.1 and 0.8, respectively. Then, the importance of the word “playing” would be associated with 0.8.

By calling MatchWords, in lines 5-6, BTI identifies word pairs from both paragraphs that share the most similar semantics. Specifically, for each word  $w_i^1 \in w^1$ , the function retrieves a matched word  $w_j^2 \in w^2$  that maximizes the similarity score between the aggregated latent representation of the words

$$w_{i^*}^2 := \arg \max_{w_j^2 \in w^2} C(\widehat{w}_i^1, \widehat{w}_j^2) \quad (5)$$

where  $\widehat{w}_i^1 \in \widehat{w}^1$  and  $\widehat{w}_j^2 \in \widehat{w}^2$  are the means of the latent tokens associated with the words  $w_i^1$  and  $w_j^2$ , respectively.

In addition to conducting matches between word pairs, the MatchWords function calculates a *word-pair score* for each pair. The word-pair score represents the accumulated importance of the pair and is defined as the multiplication of the word scores of both words along with the cosine similarity between the latent representation of the words. Formally, the word-pair score of the pair  $(w_i^1, w_j^2)$  can be written as:

$$U(w_i^1, w_j^2) := c^{ij} \cdot s_i^1 \cdot s_j^2 \quad (6)$$

where  $c^{ij}$  is the cosine similarity between the embeddings of  $w_i^1$ ,  $w_j^2$ , and  $s_i^1$ ,  $s_j^2$  are the saliency scores of the words  $w_i^1$  and  $w_j^2$ , respectively.

In line 7, BTI calls the TopWords function, which retrieves a sub-sequence of the most important word-pairs by clustering the word-pairs scores, and identifying the top-performing clusters. For retrieving the most important word-pairs, we run the MeanShift algorithm [21] on the set of word-pairs scores, to obtain the modes of the underlying distribution. MeanShift is a clustering algorithm that reveals the number of clusters in a given data and retrieves the corresponding centroid for each detected cluster. In our case, MeanShift is applied to the 1D data of all  $U(w_i^1, w_j^2)$  and identifies the subsets of the most important pairs, as the cluster associated with the top\_k centroids. In BTI, top\_k is a predefined hyperparameter. The detected most important word-pairs are retrieved as a sequence, which can be then visualized to interpret the similarity between the given two paragraphs.

## 4 EXPERIMENTS

We first demonstrate BTI’s ability to explain the similarity between items with similar descriptions, evaluated on a fashion and wine reviews<sup>3</sup> datasets, comprising ~1000 and ~120K items, respectively. The items from both datasets contain textual descriptions in the form of single paragraphs. In our experiments, we train a separate RecoBERT [34] model for each dataset. RecoBERT is a BERT-based model trained for item similarity by optimizing a cosine loss objective and a standard language model. The choice of RecoBERT stems from its ability to effectively score the similarity between two bodies of text, and since it does not require similarity labels for training.

RecoBERT training begins by initializing the model with a pre-trained BERT model and continues training by feeding the model with title-description pairs, extracted from the items in the dataset. The training objective of RecoBERT comprises a standard masked language model (similar to BERT) along with a title-description model, which enforces the model to embed item descriptions under a well-defined metric (such as the cosine function). Specifically, RecoBERT optimizes the BERT-based backbone model to embed text pairs extracted from the same item as vectors pointing to the same direction, while text pairs sampled from different items are reinforced to have in opposite directions.

<sup>3</sup><https://www.kaggle.com/zynicide/wine-reviews>

(a)	<p>0.81</p> <p>Fine-knit <b>gloves</b> in soft fabric with ribbed cuffs. Tops of thumb, index, and middle fingers in <b>touchscreen-compatible</b> fabric.</p> <p>1.0</p>	<p><b>matched-words</b></p> <p><b>Gloves, Gloves</b></p> <p><b>smartphone-friendly, touchscreen-compatible</b></p>	<p><b>Word similarity</b></p> <p><b>(0.98)</b></p> <p><b>(0.83)</b></p>	<p><b>Word-pair score</b></p> <p><b>(0.25)</b></p> <p><b>(0.83)</b></p>
	<p>0.31</p> <p>Running <b>gloves</b> with uppers in windproof functional fabric. Wide ribbing at cuffs, printed reflective detail at top, and small key pocket at back of one glove with concealed zip. Top of thumb and index finger made from <b>smartphone-friendly</b> material. Unlined</p> <p>1.0</p>			
(b)	<p>0.29 0.47</p> <p>Running <b>shirt</b> in fast-drying functional fabric with taped details. Back section in <b>ventilating</b> mesh and long raglan sleeves with thumbholes at cuffs.</p> <p>1.0</p>	<p><b>matched-words</b></p> <p><b>shirt, shirt</b></p> <p><b>Running, sports</b></p> <p><b>ventilating, breathable</b></p>	<p><b>Word similarity</b></p> <p><b>(0.95)</b></p> <p><b>(0.84)</b></p> <p><b>(0.82)</b></p>	<p><b>Word-pair score</b></p> <p><b>(0.30)</b></p> <p><b>(0.11)</b></p> <p><b>(0.56)</b></p>
	<p>0.41 0.67 0.68</p> <p>CONSCIOUS. Long-sleeved <b>sports shirt</b> in fast-drying, <b>breathable</b> functional fabric. Overlocked seams for improved comfort. Slim fit. Made partly from recycled polyester.</p>			
(c)	<p>0.27 0.31</p> <p>A <b>light</b> color and stony aromas of minerals and green <b>citrus</b> foretell a light, fresh and balanced palate. Briny green melon and underripe peach flavors finish clean and minerally, but that's as far as this standard <b>Viura</b> goes.</p> <p>0.92</p>	<p><b>matched-words</b></p> <p><b>light, translucent</b></p> <p><b>Viura, Viura</b></p> <p><b>citrus, citrusy</b></p>	<p><b>Word similarity</b></p> <p><b>(0.91)</b></p> <p><b>(0.99)</b></p> <p><b>(0.88)</b></p>	<p><b>Word-pair score</b></p> <p><b>(0.28)</b></p> <p><b>(0.32)</b></p> <p><b>(0.17)</b></p>
	<p>0.65</p> <p>A <b>translucent</b> color is backed by simple but clean aromas of wet stones and lime. In the mouth, this <b>Viura</b> is <b>citrusy</b> and fresh. Flavors of tangerine, scallion and green herbs fade on a light easy finish.</p> <p>0.87 0.39</p>			

**Figure 3: BTI results for explaining item similarities in the fashion (a-b) and wines (c) datasets. Each sample comprises two paragraphs: (1) the seed item description (top left), and (2) the description of the most similar item w.r.t. the seed (bottom left). The words retrieved by BTI are associated with saliency scores (shown next to each word). The “matched-words” column depicts the word-pairs chosen by BTI. The “word similarity” column presents the cosine scores between the word pairs. The “word-pair score” column exhibits the score from Eq.6.**

Given a trained model, we infer item-to-item similarities for each dataset by propagating all item descriptions through the specialized RecoBERT model. For each item, we extract a feature vector, as presented in Eq. 1. Then, given a seed item  $s$ , we calculate the cosine similarity between  $F_s$  and the feature vectors of all the other items in the dataset. The *candidate* item that maximizes the cosine similarity is retrieved as the *most similar item*. Finally, in order to interpret the similarity between each seed and candidate item, we employ BTI on the descriptions of both.

Figure 3 presents the interpretations of BTI for three representative seed-candidate items from the fashion and wine datasets. In the first sample, comprising two paragraphs of two glove items, BTI highlights the words “gloves” in both items, which indicates the type of the item, as well as the phrases “touchscreen-compatible”

and “smartphone-friendly”, that strongly explain the similarity between the items. For the second sample, BTI highlights the category of both items (“shirt”) and other key characteristics including “running” and “sports”, as well as “ventilating” and “breathable”, that strongly correlate. The third sample in the figure, consists of two white wine items from the wines dataset. For this sample, BTI highlights the variety of wine grape (“Viura”), the color of both wines (“light”, “translucent”) as well as a dominant flavor in both items (“citrus”, “citrusy”).

By obtaining a faithful interpretation for the similarity between paragraphs that relies on intermediate representations extracted from the model, BTI reveals the reasoning process behind RecoBERT’s embedding mechanism. Importantly, any use of other techniques for interpreting paragraph similarities that do not utilize RecoBERT’s intermediate representations would be independent

(a)	straight-cut jeans shirt with collar. Buttons at front, open chest pocket, <b>and</b> yoke at back with <b>pleat</b> . Long sleeves with buttons at <b>cuffs</b> . <b>Rounded</b> hem, slightly longer at back. 0.48 0.78 0.66 0.55	<b>Seed, candidate</b>	<b>Word similarity</b>	<b>Word-pair score</b>
		<b>and, and</b>	(0.98)	(0.352)
		<b>cuffs, cuffs</b>	(0.853)	(0.316)
		<b>pleat, cuffs</b>	(0.771)	(0.402)
		<b>Rounded, Rounded</b>	(0.791)	(0.148)
(b)	straight-cut <b>jeans</b> <b>shirt</b> with collar. Buttons at front, open chest pocket, and yoke at back with <b>pleat</b> . Long sleeves with buttons at <b>cuffs</b> . <b>Rounded</b> hem, slightly longer at back. 1.0 0.25	<b>Seed, candidate</b>	<b>Word similarity</b>	<b>Word-pair score</b>
		<b>shirt, shirt</b>	(0.945)	(0.074)
		<b>jeans, denim</b>	(0.986)	(0.986)
(c)	<b>CONSCIOUS</b> . Crew-neck T-shirts in <b>soft</b> organic cotton <b>jersey</b> . Regular fit. 0.92 0.77 0.82 1.0 0.77 0.36	<b>matched-words</b>	<b>Word similarity</b>	<b>Word-pair score</b>
		<b>soft, soft</b>	(0.808)	(0.357)
		<b>jersey, jersey</b>	(0.945)	(0.469)
		<b>Regular, Regular</b>	(0.828)	(0.510)
		<b>Regular, CONSCIOUS</b>	(0.805)	(0.296)
			(0.755)	(0.4533)
			(0.865)	(0.2930)
(d)	<b>CONSCIOUS</b> . Crew-neck <b>T-shirts</b> in soft organic cotton <b>jersey</b> . Regular fit. 0.71 0.69 0.63	<b>matched-words</b>	<b>Word similarity</b>	<b>Word-pair score</b>
		<b>jersey, jersey</b>	(0.997)	(0.111)
		<b>T-shirts, T-shirt</b>	(0.798)	(0.574)
		<b>Regular, Regular</b>	(1.0)	(0.097)
	<b>T-shirt</b> in soft cotton <b>jersey</b> . <b>Regular</b> fit. 1.0 0.16 0.15			

**Figure 4: Representative results for the parameter randomization test of BTI applied on a randomly initialized network (a,c) and BTI applied to the pre-trained weights (b,d).**

of the model weights and, therefore, will not assess the sanity of the model. This is not the case in BTI, which strongly relies on the model intermediate representations, and therefore, can assess the validity of the model. Due to the above property, BTI can allow researchers to debug their language models by analyzing the embeddings of similar paragraphs, even when similarity labels do not exist.

#### 4.1 Sanity Test

To assess the validity of BTI for explanations, we conduct the *parameter randomization* sanity test from [1]. This test uses the explainability method twice, once with random weights and once with the pre-trained weights.

Fig. 4 exhibits two representative samples processed twice by BTI. In the first application, BTI is applied with a randomly initialized

Model	MOS
(i) BTI (last layer)	2.6 ± 0.5
(ii) BTI (activations)	2.4 ± 0.6
(iii) BTI (gradients)	3.9 ± 0.3
TF-IDF-W2V	2.5 ± 0.5
IG	3.5 ± 0.4
VG	3.6 ± 0.5
BTI	<b>4.3 ± 0.3</b>

**Table 1: Human evaluations of explainability. Shown are mean and standard deviation results over all human judges.**

BERT network. In the second, BTI employs the pre-trained BERT weights. In the figure, we see that when BTI utilizes the pre-trained model, it produces semantically meaningful interpretations and fails otherwise.

Specifically, in Fig. 4(a), BTI utilizes BERT with random weights, identifies connectors (such as and), and fails by retrieving non-important word pairs (such as cuffs, pleats). For the same sample, as shown in Fig. 4(b), BTI employing the prescribed weights of the pre-trained BERT model, identifies the important words that explain the similarity between the two paragraphs by retrieving the type of fabric (denim, jeans) and the type of clothing (T-shirt), that strongly correlate both paragraphs by marking the most important mutual characteristics.

In Fig. 4(c), we observe that BTI with random weights fails to identify the category of the two items (missing the fact that the two items are T-shirts), and puts attention on two dot tokens. These problems are not apparent when BTI is applied on the trained model, for which, as can be seen in Fig. 4(d), BTI highlights the category of the item, avoids non-important punctuations, and focus on the fabric and style of the two items.

## 4.2 Human Evaluations of Explainability

The compared baselines are Vanilla Gradients (VG), Integrated Gradients (IG) [45], and a TF-IDF based method (denoted by TF-IDF-W2V).

- Vanilla Gradients (VG) - This method interprets the gradient of the loss with respect to each token as the token importance.
- Integrated Gradients (IG) - This method define an input baseline  $x'$ , which represents an input absent from information. We follow [47] and set the sequence of all zero embeddings as the input baseline. For a given input sentence  $x$ , word importance is defined by the integration of gradients along the path from the baseline to the given input. IG requires multiple feed-forward to generate the explainability of each sentence.
- TF-IDF-W2V - As a baseline method, we consider an alternative model to the word-pair scoring from Eq. 6:

$$\Lambda(w_i^1, w_j^2) := T(w_i^1)T(w_j^2)C(W(w_i^1), W(w_j^2))$$

where  $T$  and  $W$  are the TF-IDF scoring function and the word-to-vector mapping obtained by a pretrained word2vec (W2V) model [36], respectively. Hence, we dub this method TF-IDF-W2V. We see that  $\Lambda$  incorporates both the general words *importance* (captured by TF-IDF scores) as well as their semantic relatedness (captured by W2V).

Table 1 presents an ablation study for BTI and a comparison with vanilla gradients (VG), integrated gradients (IG), and TF-IDF-W2V on the fashion dataset. For the ablation, the following variants of BTI are considered: (i) utilizing the gradients and activations of the last BERT layer instead of the first one. (ii) using token-saliency scores based on the activation maps alone, and (iii) using scores solely based on gradients. The last two variants eliminate the Hadamard multiplication in Eq. 4, utilizing one variable at a time.

To compare BTI with VG, and IG, we replace the score being differentiated by the cosine similarity score (rather than the class logit). Since the above methods are not *specific*, i.e., they produce intensity scores for all words in the paragraphs, the comparison is applied via scoring the correlation of the most highlighted words, retrieved by each method, with the human perception.

To assess our full method’s performance against other alternatives and compare it to the ablation variants above, we report interpretation scoring, using a 5-point-scale Mean Opinion Score (MOS), conducted by five human judges. The same test set, comprising 100 samples, was ranked for all four BTI variants (full method and three baselines) and three baselines above. The scoring was performed blindly, and the samples were randomly shuffled. Each sample interpretation was ranked on a scale of 1 to 5, indicating poor to excellent performance.

The results in Tab. 1, highlight the superiority of BTI compared to other alternatives, indicating a better correlation with human perception. As for the ablation, the results indicate the importance of utilizing the gradients on the embedding layer from Eq. 2 as described in this paper and emphasize the importance of the multiplication between gradient and activations.

## 5 SUMMARY

We introduce the BTI method for interpreting the similarity between paragraph pairs. BTI can be applied to various natural language tasks, such as explaining text-based item recommendations. The effectiveness of BTI is demonstrated over two datasets, comprising long and complex paragraphs. Additionally, throughout extensive human evaluations, we conclude that BTI can produce explanations that correlate better with human perception. For completeness, we show that BTI passes a sanity test, commonly used in the computer vision community, that estimates the reliability of explainability methods.

Finally, we believe that BTI can expedite the research in the domain of language models by identifying failure modes in transformer-based language models and assessing deployable language models’ reliability.

## REFERENCES

- [1] Julius Adebayo, Justin Gilmer, Michael Muelly, Ian Goodfellow, Moritz Hardt, and Been Kim. 2018. Sanity Checks for Saliency Maps. arXiv:1810.03292 [cs.CV]
- [2] Vijay Arya, Rachel KE Bellamy, Pin-Yu Chen, Amit Dhurandhar, Michael Hind, Samuel C Hoffman, Stephanie Houde, Q Vera Liao, Ronny Luss, Aleksandra Mojsilović, et al. 2019. One explanation does not fit all: A toolkit and taxonomy of ai explainability techniques. *arXiv preprint arXiv:1909.03012* (2019).
- [3] Oren Barkan. 2017. Bayesian neural word embedding. In *Thirty-First AAAI Conference on Artificial Intelligence*.
- [4] Oren Barkan, Omri Armstrong, Amir Hertz, Avi Caciularu, Ori Katz, Itzik Malkiel, and Noam Koenigstein. 2021. GAM: Explainable Visual Similarity and Classification via Gradient Activation Maps. In *Proceedings of the ACM International Conference on Information & Knowledge Management (CIKM)*.
- [5] Oren Barkan, Yael Brumer, and Noam Koenigstein. 2016. Modelling Session Activity with Neural Embedding. In *RecSys Posters*.
- [6] Oren Barkan, Avi Caciularu, Ori Katz, and Noam Koenigstein. 2020. Attentive item2vec: Neural attentive user representations. In *IEEE International Conference on Acoustics, Speech and Signal Processing (ICASSP)*.
- [7] Oren Barkan, Avi Caciularu, Idan Rejwan, Ori Katz, Jonathan Weill, Itzik Malkiel, and Noam Koenigstein. 2020. Cold item recommendations via hierarchical item2vec. In *2020 IEEE International Conference on Data Mining (ICDM)*. IEEE, 912–917.
- [8] Oren Barkan, Avi Caciularu, Idan Rejwan, Ori Katz, Jonathan Weill, Itzik Malkiel, and Noam Koenigstein. 2021. Representation Learning via Variational Bayesian Networks. In *Proceedings of the ACM International Conference on Information & Knowledge Management (CIKM)*.
- [9] Oren Barkan, Yonatan Fuchs, Avi Caciularu, and Noam Koenigstein. 2020. Explainable recommendations via attentive multi-persona collaborative filtering. In *ACM Conference on Recommender Systems (RecSys)*.
- [10] Oren Barkan, Edan Hauan, Avi Caciularu, Ori Katz, Itzik Malkiel, Omri Armstrong, and Noam Koenigstein. 2021. Grad-SAM: Explaining Transformers via Gradient Self-Attention Maps. In *Proceedings of the ACM International Conference on Information & Knowledge Management (CIKM)*.
- [11] Oren Barkan, Roy Hirsch, Ori Katz, Avi Caciularu, Jonathan Weill, and Noam Koenigstein. 2021. Cold Item Integration in Deep Hybrid Recommenders via Tunable Stochastic Gates. In *2021 IEEE International Conference on Data Mining (ICDM)*. IEEE, 994–999.
- [12] Oren Barkan, Roy Hirsch, Ori Katz, Avi Caciularu, Yoni Weill, and Noam Koenigstein. 2021. Cold Start Revisited: A Deep Hybrid Recommender with Cold-Warm Item Harmonization. In *ICASSP 2021-2021 IEEE International Conference on Acoustics, Speech and Signal Processing (ICASSP)*. IEEE, 3260–3264.
- [13] Oren Barkan, Ori Katz, and Noam Koenigstein. 2020. Neural Attentive Multi-view Machines. In *IEEE International Conference on Acoustics, Speech and Signal Processing (ICASSP)*.
- [14] Oren Barkan and Noam Koenigstein. 2016. Item2vec: neural item embedding for collaborative filtering. In *2016 IEEE 26th International Workshop on Machine Learning for Signal Processing (MLSP)*. IEEE, 1–6.
- [15] Oren Barkan, Noam Koenigstein, Eylon Yogev, and Ori Katz. 2019. CB2CF: A Neural Multiview Content-to-Collaborative Filtering Model for Completely Cold Item Recommendations. In *Proceedings of the 13th ACM Conference on Recommender Systems (Copenhagen, Denmark) (RecSys '19)*. Association for Computing Machinery, New York, NY, USA, 228–236. <https://doi.org/10.1145/3298689.3347038>
- [16] Oren Barkan, Noam Razin, Itzik Malkiel, Ori Katz, Avi Caciularu, and Noam Koenigstein. 2020. Scalable attentive sentence pair modeling via distilled sentence embedding. In *Proceedings of the Conference on Artificial Intelligence (AAAI)*.
- [17] Oren Barkan, Idan Rejwan, Avi Caciularu, and Noam Koenigstein. 2020. Bayesian Hierarchical Words Representation Learning. In *Proceedings of the Annual Meeting of the Association for Computational Linguistics (ACL)*.
- [18] Solon Barocas, Andrew D Selbst, and Manish Raghavan. 2020. The hidden assumptions behind counterfactual explanations and principal reasons. In *Proceedings of the 2020 Conference on Fairness, Accountability, and Transparency*. 80–89.
- [19] Hila Chefer, Shir Gur, and Lior Wolf. 2021. Generic Attention-model Explainability for Interpreting Bi-Modal and Encoder-Decoder Transformers. *arXiv preprint arXiv:2103.15679* (2021).
- [20] Hila Chefer, Shir Gur, and Lior Wolf. 2021. Transformer interpretability beyond attention visualization. In *Proceedings of the IEEE/CVF Conference on Computer Vision and Pattern Recognition*. 782–791.
- [21] Dorin Comaniciu and Peter Meer. 2002. Mean shift: A robust approach toward feature space analysis. *IEEE Transactions on Pattern Analysis & Machine Intelligence* (2002), 603–619.
- [22] Jacob Devlin, Ming-Wei Chang, Kenton Lee, and Kristina Toutanova. 2019. BERT: Pre-training of Deep Bidirectional Transformers for Language Understanding. In *Proceedings of the 2019 Conference of the North American Chapter of the Association for Computational Linguistics: Human Language Technologies (ACL)*.
- [23] Jacob Devlin, Ming-Wei Chang, Kenton Lee, and Kristina Toutanova. 2019. BERT: Pre-training of Deep Bidirectional Transformers for Language Understanding. arXiv:1810.04805 [cs.CL]
- [24] Finale Doshi-Velez and Been Kim. 2017. Towards a rigorous science of interpretable machine learning. *arXiv preprint arXiv:1702.08608* (2017).
- [25] Javid Ebrahimi, Anyi Rao, Daniel Lowd, and Dejing Dou. 2018. HotFlip: White-Box Adversarial Examples for Text Classification. arXiv:1712.06751 [cs.CL]
- [26] Shi Feng, Eric Wallace, Mohit Iyyer, Pedro Rodriguez, Alvin Grissom II, and Jordan L. Boyd-Graber. 2018. Right Answer for the Wrong Reason: Discovery and Mitigation. *CoRR abs/1804.07781* (2018). arXiv:1804.07781 <http://arxiv.org/abs/1804.07781>
- [27] Leilani H Gilpin, David Bau, Ben Z Yuan, Ayesha Bajwa, Michael Specter, and Lalana Kagal. 2018. Explaining explanations: An overview of interpretability of machine learning. In *2018 IEEE 5th International Conference on data science and advanced analytics (DSAA)*. IEEE, 80–89.
- [28] Dvir Ginzburg, Itzik Malkiel, Oren Barkan, Avi Caciularu, and Noam Koenigstein. 2021. Self-Supervised Document Similarity Ranking via Contextualized Language Models and Hierarchical Inference. In *Findings of the Association for Computational Linguistics: ACL-IJCNLP 2021*. Association for Computational Linguistics, Online, 3088–3098. <https://doi.org/10.18653/v1/2021.findings-acl.272>
- [29] Bryce Goodman and Seth Flaxman. 2016. EU regulations on algorithmic decision-making and a “right to explanation”. In *ICML workshop on human interpretability in machine learning (WHI 2016)*, New York, NY. <http://arxiv.org/abs/1606.08813> v1.
- [30] Benjamin Hoover, Hendrik Strobelt, and Sebastian Gehrmann. 2019. exBERT: A Visual Analysis Tool to Explore Learned Representations in Transformers Models. arXiv:1910.05276 [cs.CL]
- [31] Todd Kulesza, Simone Stumpf, Margaret Burnett, Weng-Keen Wong, Yann Riche, Travis Moore, Ian Oberst, Amber Shinsel, and Kevin McIntosh. 2010. Explanatory debugging: Supporting end-user debugging of machine-learned programs. In *2010 IEEE Symposium on Visual Languages and Human-Centric Computing*. IEEE, 41–48.
- [32] Tao Lei, Regina Barzilay, and Tommi Jaakkola. 2016. Rationalizing Neural Predictions. arXiv:1606.04155 [cs.CL]
- [33] Yinhan Liu, Myle Ott, Naman Goyal, Jingfei Du, Mandar Joshi, Danqi Chen, Omer Levy, Mike Lewis, Luke Zettlemoyer, and Veselin Stoyanov. 2019. RoBERTa: A Robustly Optimized BERT Pretraining Approach. arXiv:1907.11692 [cs.CL]
- [34] Itzik Malkiel, Oren Barkan, Avi Caciularu, Noam Razin, Ori Katz, and Noam Koenigstein. 2020. RecoBERT: A Catalog Language Model for Text-Based Recommendations. In *Findings of the Association for Computational Linguistics: EMNLP 2020*. Association for Computational Linguistics, Online, 1704–1714. <https://doi.org/10.18653/v1/2020.findings-emnlp.154>
- [35] Itzik Malkiel and Lior Wolf. 2021. Maximal Multiverse Learning for Promoting Cross-Task Generalization of Fine-Tuned Language Models. In *Proceedings of the 16th Conference of the European Chapter of the Association for Computational Linguistics: Main Volume*. Association for Computational Linguistics, Online, 187–199. <https://doi.org/10.18653/v1/2021.eacl-main.14>
- [36] Tomas Mikolov, Ilya Sutskever, Kai Chen, Greg S Corrado, and Jeff Dean. 2013. Distributed representations of words and phrases and their compositionality. In *Advances in neural information processing systems (NIPS)*.
- [37] Jeffrey Pennington, Richard Socher, and Christopher Manning. 2014. Glove: Global vectors for word representation. In *Proceedings of the 2014 conference on empirical methods in natural language processing (EMNLP)*. 1532–1543.
- [38] Marco Tulio Ribeiro, Sameer Singh, and Carlos Guestrin. 2016. “Why should I trust you?” Explaining the predictions of any classifier. In *Proceedings of the 22nd ACM SIGKDD international conference on knowledge discovery and data mining*. 1135–1144.
- [39] Marco Tulio Ribeiro, Sameer Singh, and Carlos Guestrin. 2016. “Why Should I Trust You??: Explaining the Predictions of Any Classifier. In *Proceedings of the 22nd ACM SIGKDD International Conference on Knowledge Discovery and Data Mining (San Francisco, California, USA) (KDD '16)*. Association for Computing Machinery, New York, NY, USA, 1135–1144. <https://doi.org/10.1145/2939672.2939778>
- [40] Ruslan Salakhutdinov and Andriy Mnih. 2008. Bayesian probabilistic matrix factorization using Markov chain Monte Carlo. In *Proceedings of the 25th international conference on Machine learning*. ACM, 880–887.
- [41] Andrew Selbst and Julia Powles. 2018. “Meaningful Information” and the Right to Explanation. In *Conference on Fairness, Accountability and Transparency*. PMLR, 48–48.
- [42] Andrew D Selbst and Solon Barocas. 2018. The intuitive appeal of explainable machines. *Fordham L. Rev.* 87 (2018), 1085.
- [43] Jost Tobias Springenberg, Alexey Dosovitskiy, Thomas Brox, and Martin Riedmiller. 2015. Striving for Simplicity: The All Convolutional Net. arXiv:1412.6806 [cs.LG]

- [44] Fei Sun, Jun Liu, Jian Wu, Changhua Pei, Xiao Lin, Wenwu Ou, and Peng Jiang. 2019. BERT4Rec: Sequential Recommendation with Bidirectional Encoder Representations from Transformer. In *Proceedings of the ACM International Conference on Information and Knowledge Management (CIKM)*.
- [45] Mukund Sundararajan, Ankur Taly, and Qiqi Yan. 2017. Axiomatic attribution for deep networks. In *International Conference on Machine Learning*. PMLR, 3319–3328.
- [46] Ashish Vaswani, Noam Shazeer, Niki Parmar, Jakob Uszkoreit, Llion Jones, Aidan N. Gomez, Lukasz Kaiser, and Illia Polosukhin. 2017. Attention Is All You Need. *arXiv:1706.03762* [cs.CL]
- [47] Eric Wallace, Jens Tuyls, Junlin Wang, Sanjay Subramanian, Matt Gardner, and Sameer Singh. 2019. AllenNLP Interpret: A Framework for Explaining Predictions of NLP Models. *arXiv:1909.09251* [cs.CL]
- [48] Yonghui Wu, Mike Schuster, Zhifeng Chen, Quoc V Le, Mohammad Norouzi, Wolfgang Macherey, Maxim Krikun, Yuan Cao, Qin Gao, Klaus Macherey, et al. 2016. Google’s neural machine translation system: Bridging the gap between human and machine translation. *arXiv preprint arXiv:1609.08144* (2016).
- [49] Hu Xu, Bing Liu, Lei Shu, and Philip S Yu. 2019. Bert post-training for review reading comprehension and aspect-based sentiment analysis. *arXiv preprint arXiv:1904.02232* (2019).
- [50] Jason Yosinski, Jeff Clune, Anh Nguyen, Thomas Fuchs, and Hod Lipson. 2015. Understanding Neural Networks Through Deep Visualization. *arXiv:1506.06579* [cs.CV]
- [51] Matthew D Zeiler and Rob Fergus. 2014. Visualizing and understanding convolutional networks. In *European conference on computer vision*. Springer, 818–833.
- [52] Matthew D Zeiler, Graham W Taylor, and Rob Fergus. 2011. Adaptive deconvolutional networks for mid and high level feature learning. In *2011 International Conference on Computer Vision*. IEEE, 2018–2025.
- [53] Zhengli Zhao, Dheeru Dua, and Sameer Singh. 2017. Generating natural adversarial examples. *arXiv preprint arXiv:1710.11342* (2017).